
A FAST REDUCED ORDER METHOD FOR LINEAR PARABOLIC INVERSE SOURCE PROBLEMS

A PREPRINT

Yuxuan Huang
Mathematical sciences department
Carnegie Mellon University
Pittsburgh, PA 15213
yuxuanhu@andrew.cmu.edu

Yangwen Zhang
Mathematical sciences department
Carnegie Mellon University
Pittsburgh, PA 15213
yangwenz@andrew.cmu.edu

June 12, 2023

ABSTRACT

In this paper, we propose a novel, computationally efficient reduced order method to solve linear parabolic inverse source problems. Our approach provides accurate numerical solutions without relying on specific training data. The forward solution is constructed using a Krylov sequence, while the source term is recovered via the conjugate gradient (CG) method. Under a weak regularity assumption on the solution of the parabolic partial differential equations (PDEs), we establish convergence of the forward solution and provide a rigorous error estimate for our method. Numerical results demonstrate that our approach offers substantial computational savings compared to the traditional finite element method (FEM) and retains equivalent accuracy.

Keywords Inverse source problems · heat equation · reduced order method · finite element method · stochastic error estimate

1 Introduction

The study of parabolic inverse source problems has received considerable attention in the field of numerical analysis over the past decades. These problems aim to determine an unknown source term from final time observations of the solution of a time-dependent partial differential equation (PDE). Canonically, the forward problem is to determine the solution of the parabolic PDE given the source term and boundary conditions, while the inverse problem is to determine the source term from final time observations of the solution. To solve an inverse problem numerically, we need to compute many forward problems in the process. The parabolic inverse source problem arises in many applications, including contaminant transport in porous media [4], heat conduction in materials [1], and tumor growth modeling [9]. However, obtaining numerical solutions is challenging due to the ill-posedness of the inverse problem [1] and the high computational cost of solving the forward problem [2].

Traditionally, finite element methods (FEM) have been widely used to solve the parabolic inverse source problem. FEM discretizes the PDE and its solution into a system of algebraic equations, which can be solved using iterative methods such as the conjugate gradient method [10]. Although FEM can achieve accurate results, it requires many unknowns and leads to high computational costs and memory storage requirements.

Recently, reduced order methods (ROMs) have been proposed as an alternative approach to solving the parabolic inverse source problem. The main idea of ROMs is to find a low-dimensional basis for the solution space and use this basis to represent the solution of the PDE. This leads to significant computational savings compared to FEM [12].

One popular ROM for the parabolic inverse source problem is the proper orthogonal decomposition (POD) method. POD approximates the solution space by constructing an orthonormal basis from a set of snapshots of the solution. This basis can be used to represent the solution of the PDE and reduce the computational cost. But POD's reduced order basis heavily depends on the specific PDE data. In an inverse problem where the actual source term is very different

from the example used to construct the POD basis, the results can be either a reasonable approximation or an absurd deviation [7]. To compensate for the narrow specificity of POD, hybrid ROMs are developed to take advantage of both POD and full-order methods (FOMs) such as FEM [5]. Nevertheless, their computational savings are not remarkable in the parabolic inverse source problems.

To address the aforementioned deficits in different methods, we offer a novel approach that is computationally economical and insensitive to changes in data. In this work, we study our proposed method under a practically physical scenario. The rest of the paper is organized as follows. In Section 2, we introduce the setting of the linear parabolic inverse source problem. In Section 3, we provide the specific implementation of the finite element method and our reduced order method. In section 4, we prove the convergence of the forward solution and present a stochastic error estimate. In section 5, we demonstrate numerical results to compare our method with standard FEM. Lastly, we discuss the limitation and future directions of our work in Section 6.

2 Formulation of the inverse problem

Because linear parabolic inverse problems are well-studied and suitable for comparison purposes, we choose to focus on this type of inverse source problems in this paper. We consider the PDE system governed by the following state equation:

$$\begin{cases} u_t - \Delta u = f, & \text{in } \Omega \times (0, T] \\ u(\cdot, t) = 0, & \text{on } \partial\Omega \times (0, T] \\ u(\cdot, 0) = 0, & \text{in } \Omega \end{cases} \quad (2.1)$$

Where $\emptyset \neq \Omega \subset \mathbb{R}^d (d = 1, 2, 3)$ is a bounded domain, $T > 0$ is the terminal time.

Let u be the solution and f be a time-independent source term of the state equation (2.1). We define the forward operator $\mathcal{S} : L^2(\Omega) \rightarrow L^2(\Omega)$ by $\mathcal{S}f = u(\cdot, T)$. In the linear parabolic inverse source problem, $f \in L^2(\Omega)$ is an unknown source term that we want to reconstruct based on the measurement of final time solution $u(\cdot, T)$.

In this work, we assume that the measurement of $u(\cdot, T)$ are collected point-wisely over a set of uniformly distributed sensors located at $\{x_i\}_{i=1}^n$ over Ω (e.g. [ref]). To account for the uncertainty of natural noise and measurement errors, we apply independent Gaussian random noise to each sensor. We denote the noise as $\{e_i\}_{i=1}^n$. They are independent and identically distributed (i.i.d.) random variables with Gaussian distribution $N(0, \epsilon^2)$ for some small $\epsilon > 0$. So the actual measurement takes the form $m_i = \mathcal{S}f^*(x_i) + e_i$, $i = 1, 2, \dots, n$, where $f^* \in L^2(\Omega)$ is the true source term of the problem.

For any $u, v \in C(\bar{\Omega})$ and $y \in \mathbb{R}^n$ we define the inner product

$$(u, v)_n = \frac{1}{n} \sum_{i=1}^n u(x_i)v(x_i), \quad (y, v)_n = \frac{1}{n} \sum_{i=1}^n y_i v(x_i)$$

and the empirical norm

$$\|u\|_n = \left(\frac{1}{n} \sum_{i=1}^n u^2(x_i) \right)^{1/2}$$

Now, we define the linear parabolic inverse source problem as to reconstruct a unknown source term f^* from the noisy final time measurement data $m = (m_1, m_2, \dots, m_n)^T \in \mathbb{R}^n$. We implement a realistic approach for this problem by optimizing the mean-square error with a regularization term. The approximation solution is hence computed from the following optimization problem:

$$\min_{f \in L^2(\Omega)} \frac{1}{2} \|\mathcal{S}f - m\|_n^2 + \frac{\lambda_n}{2} \|f\|_{L^2(\Omega)}^2 \quad (2.2)$$

where λ_n is the regularization parameter.

Additionally, to solve the inverse problem we need the adjoint equation

$$\begin{cases} y_t - \Delta y = g, & \text{in } \Omega \times (0, T] \\ y(\cdot, t) = 0, & \text{on } \partial\Omega \times (0, T] \\ y(\cdot, 0) = 0, & \text{in } \Omega \end{cases} \quad (2.3)$$

where $g \in L^2(\Omega)$ is time-independent. This adjoint equation is in accordance with the work of Johansson and Lesnic [8]. The elliptic operator in their assumption $\mathcal{L}u = -\sum_{i,j=1}^d \partial_{x_i}(a_{i,j}(x)\partial_{x_j}u) + \sum_{i=1}^d b_i(x)\partial_{x_i}u + c(x)u$ is set to be the

negative Laplace operator here. Then we define the adjoint forward operator $\mathcal{S}^* : L^2(\Omega) \rightarrow L^2(\Omega)$ by $\mathcal{S}^* g = y(\cdot, T)$. Note that the adjoint equation is the same as the state equation under our context.

In a previous work done by Chen et al. [3], they studied the optimal stochastic convergence of regularized finite element solutions to a more general type of parabolic inverse source problems. The following result represents the stochastic convergence with random noise with bounded variance.

Assumption 1. (Assumption 2.1 in [3]) We assume the following:

(1) There exists a constant $\beta > 1$ such that for all $u \in L^2(\Omega)$,

$$\|u\|_{L^2(\Omega)}^2 \leq C(\|u\|_n^2 + n^{-\beta} \|u\|_{L^2(\Omega)}^2), \quad \|u\|_n^2 \leq C(1 + n^{-\beta}) \|u\|_{L^2(\Omega)}^2 \quad (2.4)$$

(2) The first n eigenvalues, $0 < \eta_1 \leq \eta_2 \leq \dots \leq \eta_n$, of the eigenvalue problem

$$(\psi, v)_{L^2(\Omega)} = \eta(\mathcal{S}\psi, \mathcal{S}v)_{L^2(\Omega)} \quad \forall v \in L^2(\Omega) \quad (2.5)$$

satisfy that $\eta_k \geq Ck^\alpha$, $k = 1, 2, \dots, n$. The constant C depends only on the forward operator \mathcal{S} . And the constant α satisfies $1 \leq \alpha \leq \beta$.

Proposition 1. (Theorem 3.5 in [3]) Suppose Assumption 1 holds and $\{e_i\}_{i=1}^n$ are independent random variables satisfying $\mathbb{E}[e_i] = 0$ and $\mathbb{E}[e_i^2] \leq \sigma^2$. Let $f_n \in L^2(\Omega)$ be the solution to the minimization problem (2.2). Then there exists constants $\lambda_0 > 0$ and $C > 0$ such that the following estimates hold for all $0 < \lambda_n < \lambda_0$:

$$\mathbb{E}[\|\mathcal{S}f_n - \mathcal{S}f_n^*\|_n^2] \leq C\lambda_n \|f_n^*\|_{L^2(\Omega)}^2 + \frac{C\sigma^2}{n\lambda_n^{d/4}} \quad (2.6)$$

$$\mathbb{E}[\|f_n - f_n^*\|_{L^2(\Omega)}^2] \leq C\|f_n^*\|_{L^2(\Omega)}^2 + \frac{C\sigma^2}{n\lambda_n^{1+d/4}} \quad (2.7)$$

Since our problem of interest is a linear parabolic inverse source problem and our noise is i.i.d. Gaussian random with variance σ^2 , the above proposition applies to this case.

3 Implementation of numerical solvers

The algorithm consists of forward and the backward processes. The forward process solves the state and the adjoint equations. The backward process employs the results of the forward process and solves for the true source term. For simplicity, we denote the Euclidean norm $\|\cdot\|_{L^2(\Omega)} = \|\cdot\|_2$.

3.1 The backward process

In this part, we illustrate the algorithm to find the approximation to the true source term.

Let $\mathcal{J}(f)$ be objective function of our optimization problem (2.2). By construction it is convex, so its minimizer is a global one. Then we use the first-order optimality condition:

$$\nabla \mathcal{J}(f) = (\mathcal{S}^* \mathcal{S} + \lambda_n \mathbb{I})f - \mathcal{S}^* m \stackrel{\text{set}}{=} 0 \quad (3.1)$$

where \mathcal{S}^* is the adjoint operator of \mathcal{S} .

Define $A(\lambda_n) := (\mathcal{S}^* \mathcal{S} + \lambda_n \mathbb{I})$, $b(m) := \mathcal{S}^* m$, then solving the problem (2.2) is equivalent to solve $Af = b$. And hence, we implement the conjugate gradient method (CG) to find the solution. Let f_0 be an initial guess and tol be the tolerance; m is the given final time observation for the inverse source problem and λ_n is the regularization parameter.

Since we cannot directly derive the exact values for $A(\lambda_n)$ or $b(m)$ in a numerical setting, we introduce Algorithm 1. It incorporates the forward process which we will cover in the next subsection.

The inner product we use in Algorithm 1 is defined as below:

$$\forall x, y \in \mathbb{R}^n, (x, y)_M = (x, My)_2 = x^T My, \quad \|x\|_M = x^T Mx$$

Where M is the mass matrix in the finite element discretization. This is a well-defined norm since M is symmetric and positive definite (SPD) by Lemma 4 in appendix. Since we use $\|\cdot\|_n$ instead of $\|\cdot\|_M$ in our proofs, we thus prove that these two norms are equivalent in Proposition 2.

Algorithm 1 CG framework**Input:** f_0, tol, m, λ_n

```

1:  $u_0 = \text{forward\_solve}(f_0)$  ▷ This is  $Sf_0$ 
2:  $r_0 = \text{forward\_solve}(m - u_0) - \lambda_n f_0$  ▷ This is  $S^*(m) - (S^*S + \lambda_n \mathbb{I})f_0$ 
3:  $p_0 = r_0$ ;  $error = \|p_0\|_M$ 
4: while  $error \geq tol$  do
5:    $u_k = \text{forward\_solve}(p_k)$  ▷ This is  $S p_k$ 
6:    $A p_k = \text{forward\_solve}(u_k) + \lambda_n p_k$  ▷ This is  $(S^*S + \lambda_n \mathbb{I})p_k$ 
7:    $\alpha = \frac{(r_k, r_k)_M}{(p_k, A p_k)_M}$ 
8:    $f_{k+1} = f_k + \alpha p_k$ 
9:    $r_{k+1} = r_k - \alpha A p_k$ 
10:   $\beta = \frac{(r_{k+1}, r_{k+1})_M}{(r_k, r_k)_M}$ 
11:   $p_{k+1} = r_{k+1} + \beta p_k$ 
12:   $error = \|p_{k+1}\|_M$ 
13: end while
14: return  $f_{k'}$  for some  $k' \in \mathbb{N}_{\geq 0}$ 

```

Proposition 2. For a fixed $n \in \mathbb{N}$, the finite element norm $\|\cdot\|_M$ and the empirical norm $\|\cdot\|_n$ are equivalent.

Proof. By the definition of equivalency, we want to show that there exists constants $c_1, c_2 > 0$ such that for any $v \in \mathbb{R}^n$, $c_1 \|v\|_n \leq \|v\|_M \leq c_2 \|v\|_n$. By Lemma 4 in appendix, $M \in \mathbb{R}^{n \times n}$ is SPD. So by the spectral theorem, we can decompose M as such:

$$M = \sum_{i=1}^n \lambda_i p_i p_i^T$$

Where $p_i \in \mathbb{R}^n$, $\|p_i\|_2 = 1$, and $(p_i, p_j)_2 = 0 \forall 1 \leq i \neq j \leq n$. And $0 < \lambda_1 \leq \dots \leq \lambda_n$ are the eigenvalues of M . Fix any $v \in \mathbb{R}^n$,

$$\begin{aligned} \|v\|_M &= v^T M v \\ &= \sum_{i=1}^n \lambda_i (v^T p_i) (p_i^T v) \\ &= \sum_{i=1}^n \lambda_i (v^T p_i)^2 \end{aligned}$$

Let $y_i = v^T p_i$, $y = [y_1, \dots, y_n]^T$

$$= \sum_{i=1}^n \lambda_i y_i^2$$

So we have

$$\lambda_1 \sum_{i=1}^n y_i^2 \leq \sum_{i=1}^n \lambda_i y_i^2 \leq \lambda_n \sum_{i=1}^n y_i^2$$

Note that $\mathbb{I} = \sum_{i=1}^n p_i p_i^T$ (all eigenvalues are 1)

$$\sum_{i=1}^n y_i^2 = \sum_{i=1}^n v^T (p_i p_i^T) v = v^T v = \|v\|_2$$

By definition, $\|v\|_n = \frac{1}{n^{1/2}} \|v\|_2$. Therefore

$$\lambda_1 n^{1/2} \|v\|_n \leq \|v\|_M \leq \lambda_n n^{1/2} \|v\|_n$$

□

3.2 The forward process

In this part, we introduce the implementations to solve the state equation (2.1) only since the adjoint equation is essentially identical here.

3.2.1 Space-time Discretization

Given the bounded domain Ω , we specify a spatial mesh size h and select a finite element space V_h from the Sobolev space $H_0^1(\Omega)$. Then given a source term $f \in L^2(\Omega)$, the semi-discrete formulation is to find $u_h \in C^0((0, T], V_h)$ with $u_h(0) = 0$ satisfying:

$$(\partial_t u_h(t), \nu) + (\nabla u_h(t), \nabla \nu) = (f, \nu) \quad \forall \nu \in V_h, t \in (0, T] \quad (3.2)$$

Next, we specify a temporal stepsize Δt and denote $u_h^n = u_h(n \cdot \Delta t)$. So the full-discrete formulation is to find $u_h^n \in V_h$ with $u_h^0 = 0 \quad \forall n \in \{1, 2, \dots, \text{ceil}(\frac{T}{\Delta t})\}$ satisfying:

$$(\partial_t^+ u_h^n, \nu) + (\nabla u_h^n, \nabla \nu) = (f, \nu) \quad \forall \nu \in V_h \quad (3.3)$$

We replace $\nu \in V_h$ by canonical shape functions in the finite element method to formulate the matrix representation from (3.3). So we need to find $u_h^n \in V_h$ with $u_h^0 = 0 \quad \forall n \in \{1, 2, \dots, \text{ceil}(\frac{T}{\Delta t})\}$ satisfying:

$$M \partial_t^+ u_h^n + A u_h^n = b \quad (3.4)$$

Here M is the mass matrix, A is the stiffness matrix, and b is the load vector.

To derive $\partial_t^+ u_h^n$, we use a backward differentiation formula (BDF) scheme:

$$\partial_t^+ u_h^n = \begin{cases} 0 & n = 0 \\ \frac{u_h^n - u_h^{n-1}}{\Delta t} & n = 1 \\ \frac{3u_h^n - 4u_h^{n-1} + u_h^{n-2}}{2\Delta t} & n \geq 2 \end{cases} \quad (3.5)$$

3.2.2 The finite element method

Our implementation of the finite element method is conducted using the NGSolve package because it possesses high performance and yields reliable results. The package can be downloaded at <https://ngsolve.org/downloads>. The code is included in the github repository, and the link will be available in section 5.

3.2.3 The fast reduced order method

In a nutshell, our reduced order method utilizes the discretization matrices from FEM (in our case, via NGSolve) and then employs a Krylov sequence to conduct dimensional reduction. This method is more convenient and adaptable than other existing reduced order methods because it does not require extra training data to generate the reduced order basis. So this new approach can solve the inverse problem without having any prior knowledge about the true source term. See Fig.1 for a pipeline illustration.

In this paper, we provide a general idea of the ROM and a more detailed analysis of this method is given in the work of Walkington et al. [11].

Basically, we want to reduce the forward problem to a small dimension which is denoted as $\ell (\leq 10)$. So we need a reduced order basis (ROB) that retains essential information about the problem and extract a projection matrix to project the full order model (FOM) to the reduced subspace.

First, we generate a Krylov sequence based on the discretization matrices M , A and b in (3.4).

$$\mathbf{u}_h^i = \sum_{j=1}^N (u_i)_j \varphi_j, \quad u_i \in \mathbb{R}^N, \quad \varphi_j \in V_h, \quad \forall 1 \leq i \leq \ell \quad (3.6)$$

Where N is the dimension of V_h .

$$A u_1 = b, \quad A u_i = M u_{i-1} \quad \forall 2 \leq i \leq \ell \quad (3.7)$$

$$U_\ell = [u_1 | u_2 | \dots | u_\ell] \in \mathbb{R}^{N \times \ell}, \quad r = \text{rank}(U_\ell) \quad (3.8)$$

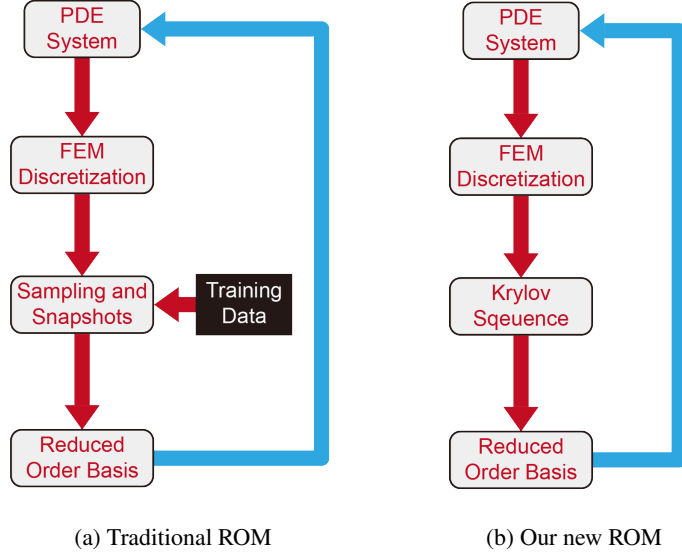


Figure 1: Pipeline comparison

Note that if needed, we can set $r = \ell$ to simplify computations.

In this paper, we use $(\nabla\varphi, \nabla\psi) = (\varphi, \psi)_V \quad \forall \varphi, \psi \in V_h$. For a complete definition of $(\cdot, \cdot)_V$, see Section 2 of [11]. To find the reduced order basis, we solve the following minimization problem:

$$\min_{\tilde{\varphi}_1, \dots, \tilde{\varphi}_r \in V_h} \sum_{j=1}^{\ell} \|\mathbf{u}_h^j - \sum_{i=1}^r (\mathbf{u}_h^j, \tilde{\varphi}_i)_V \tilde{\varphi}_i\|_V \quad \text{with } (\tilde{\varphi}_i, \tilde{\varphi}_j)_V = \delta_{ij}, \quad \forall 1 \leq i, j \leq r \leq \ell \quad (\text{P1})$$

Lemma 1. (modified Lemma 1 in [11]) The solution to (P1) is the first r eigenfunctions of $\mathcal{R} : V_h \rightarrow V_h$ where $\mathcal{R}(\varphi) = \sum_{j=1}^{\ell} (\mathbf{u}_h^j, \varphi)_V \mathbf{u}_h^j$

The proof of Lemma 1 can be found in Theorem 2.7 of [6].

Lemma 2. $\mathcal{R} = \mathcal{U}\mathcal{U}^*$, where $\mathcal{U} : \mathbb{R}^{\ell} \rightarrow V_h$ is a compact linear operator and $\mathcal{U}^* : V_h \rightarrow \mathbb{R}^{\ell}$ is the Hilbert adjoint operator. And $\mathcal{U}^*\mathcal{U}\alpha = U_{\ell}^T A U_{\ell} \alpha \quad \forall \alpha \in \mathbb{R}^{\ell}$, where A is the stiffness matrix in (3.4) and U_{ℓ} is the Krylov matrix in (3.8).

Proof. We define $\mathcal{U} : \mathbb{R}^{\ell} \rightarrow V_h$ by $\mathcal{U}\alpha = \sum_{i=1}^{\ell} \alpha_i \mathbf{u}_h^i$, where $\alpha = [\alpha_1, \alpha_2, \dots, \alpha_{\ell}]^T \in \mathbb{R}^{\ell}$. The Hilbert adjoint operator $\mathcal{U}^* : V_h \rightarrow \mathbb{R}^{\ell}$ satisfies

$$(\mathcal{U}^* \nu, \alpha)_{\mathbb{R}^{\ell}} = (\nu, \mathcal{U}\alpha)_V = \sum_{i=1}^{\ell} \alpha_i (\mathbf{u}_h^i, \nu)_V$$

This implies

$$\mathcal{U}^* \nu = [(\mathbf{u}_h^1, \nu)_V, \dots, (\mathbf{u}_h^{\ell}, \nu)_V]^T$$

So

$$\mathcal{U}\mathcal{U}^* \nu = \sum_{i=1}^{\ell} (\mathbf{u}_h^i, \nu)_V \mathbf{u}_h^i = \mathcal{R}\nu$$

We also have

$$\mathcal{U}^*\mathcal{U}\alpha = [(\mathbf{u}_h^1, \sum_{i=1}^{\ell} \alpha_i \mathbf{u}_h^i)_V, \dots, (\mathbf{u}_h^{\ell}, \sum_{i=1}^{\ell} \alpha_i \mathbf{u}_h^i)_V]^T$$

By (3.6) and the definition of the stiffness matrix A

$$(\mathbf{u}_h^i, \mathbf{u}_h^j)_V = \left(\sum_{k=1}^N (u_i)_k \varphi_k, \sum_{k=1}^N (u_j)_k \varphi_k \right)_V = u_i^T A u_j$$

Then with (3.8), we have

$$\mathcal{U}^* \mathcal{U} \alpha = \left[\sum_{i=1}^{\ell} \alpha_i u_1^T A u_i, \dots, \sum_{i=1}^{\ell} \alpha_i u_{\ell}^T A u_i \right]^T = U_{\ell}^T A U_{\ell} \alpha$$

□

Lemma 3. Denote $K_{\ell} = U_{\ell}^T A U_{\ell} \in \mathbb{R}^{\ell \times \ell}$. Let $\lambda_1(K_{\ell}) \geq \lambda_2(K_{\ell}) \geq \dots \geq \lambda_{\ell}(K_{\ell}) > 0$ be the eigenvalues of K_{ℓ} , then $\lambda_i(K_{\ell}) = \lambda_i(\mathcal{R})$, $\forall 1 \leq i \leq \ell$. Moreover, if $x_i \in \mathbb{R}^{\ell}$ and $\mathcal{U}^* \mathcal{U} x_i = \lambda_i x_i$ s.t. $\lambda_i > 0$ and x_i is orthonormal, then let $y_i = \frac{1}{\sqrt{\lambda_i}} \mathcal{U} x_i$ we have $\mathcal{U} \mathcal{U}^* y_i = \lambda_i y_i$ and y_i is orthonormal.

Proof. Here we prove a more general case, that the nonzero eigenvalues of $\mathcal{U} \mathcal{U}^*$ and $\mathcal{U}^* \mathcal{U}$ are the same. Say $\lambda \neq 0$ is an eigenvalue of $\mathcal{U} \mathcal{U}^*$ with eigenfunction $x \in V_h$. Then

$$\mathcal{U}^* \mathcal{U} (\mathcal{U}^* x) = \mathcal{U}^* (\mathcal{U} \mathcal{U}^* x) = \lambda \mathcal{U}^* x$$

So λ is an eigenvalue of $\mathcal{U}^* \mathcal{U}$ with eigenvector $\mathcal{U}^* x \in \mathbb{R}^{\ell}$. Proving the other direction uses the same process. Thus, by Lemma 2, the positive eigenvalues of K_{ℓ} and \mathcal{R} are the same.

Next, let $x_i \in \mathbb{R}^{\ell}$ and $\mathcal{U}^* \mathcal{U} x_i = \lambda_i x_i$ s.t. $\lambda_i > 0$ and x_i is orthonormal. Set $y_i = \frac{1}{\sqrt{\lambda_i}} \mathcal{U} x_i$, it is clear that y_i is orthonormal and

$$\mathcal{U} \mathcal{U}^* y_i = \frac{\lambda_i}{\sqrt{\lambda_i}} \mathcal{U} x_i = \sqrt{\lambda_i} \mathcal{U} x_i = \lambda_i y_i$$

□

Theorem 1. The solution to (P1) is $\tilde{\varphi}_i = \frac{1}{\sqrt{\lambda_i}} \mathcal{U} \psi_i$, where $\lambda_i > 0$ and ψ_i satisfies $K_{\ell} \psi_i = \lambda_i \psi_i$, $i = 1, 2, \dots, r$. And the coefficient vector of $\tilde{\varphi}_i$ is $\frac{1}{\sqrt{\lambda_i}} U_{\ell} \cdot \psi_i$.

Proof. By Lemma 3, the eigenvalues of K_{ℓ} and \mathcal{R} are the same. So let $\psi_1, \dots, \psi_r \in \mathbb{R}^{\ell}$ be the first r orthonormal eigenvectors of K_{ℓ} with eigenvalues $\lambda_1 \geq \dots \geq \lambda_r > 0$ respectively. Then let $\tilde{\varphi}_i = \frac{1}{\sqrt{\lambda_i}} \mathcal{U} \psi_i$, $\tilde{\varphi}_i$'s are the first r orthonormal eigenfunctions of $\mathcal{U} \mathcal{U}^*$. So $\tilde{\varphi}_1, \dots, \tilde{\varphi}_r$ are the solution to (P1) by Lemma 1 and Lemma 2. By the definition in Lemma 2,

$$\mathcal{U} \psi_i = \sum_{j=1}^{\ell} (\psi_i)_j \sum_{k=1}^N (u_j)_k \varphi_k = \sum_{k=1}^N \left(\sum_{j=1}^{\ell} (\psi_i)_j (u_j)_k \right) \varphi_k = \sum_{k=1}^N (U_{\ell} \cdot \psi_i)_k \varphi_k$$

Where $(U_{\ell} \cdot \psi_i)_k$ is the k th component of $U_{\ell} \cdot \psi_i \in \mathbb{R}^N$. Thus, the coefficient vector of $\tilde{\varphi}_i$ is $\frac{1}{\sqrt{\lambda_i}} U_{\ell} \cdot \psi_i$ □

We obtain the reduced order coefficient (projection) matrix Q via concatenating the coefficient vectors.

$$Q = U_{\ell} \left[\frac{\psi_1}{\sqrt{\lambda_1}} \mid \frac{\psi_2}{\sqrt{\lambda_2}} \mid \dots \mid \frac{\psi_r}{\sqrt{\lambda_r}} \right] \quad (3.9)$$

The following is our algorithm to compute the matrix Q .

Now that we obtain the coefficient matrix to generate the reduced order basis. We can compute the reduced order subspace

$$V_r = \text{span}\{\tilde{\varphi}_1, \tilde{\varphi}_2, \dots, \tilde{\varphi}_r\}$$

The reduced order formulation is a modification to (3.4), we need to find $u_r^n \in V_r$ with $u_r^0 = 0 \forall n \in \{1, 2, \dots, \text{ceil}(\frac{T}{\Delta t})\}$ satisfying:

$$M_r \partial_t^+ u_r^n + A_r u_r^n = b_r \quad (3.10)$$

where

$$M_r = Q^T M Q, \quad A_r = Q^T A Q, \quad b_r = Q^T b \quad (3.11)$$

Algorithm 2 get_matrix_Q (Algorithm 2 in [11])**Input:** M, A, b, ℓ, tol

```

1: Solve  $Au_1 = b$ 
2:  $U_1 = u_1, K_1 = u_1^T Au_1$ 
3: for  $i = 2$  to  $\ell$  do
4:   Solve  $Au_i = Mu_{i-1}$ 
5:    $U_i = [U_{i-1} | u_i]$ 
6:   if  $K_{i-1}$  is a scalar then  $\alpha = u_{i-1}^T Au_i$ 
7:   else  $\alpha = [K_{i-1}(i-1, 2:i-1) | u_{i-1}^T Au_i]$ 
8:   end if
9:    $\beta = u_i^T Au_i$ 
10:   $K_i = \begin{bmatrix} K_{i-1} & \alpha^T \\ \alpha & \beta \end{bmatrix}$ 
11:   $[\Psi, \Lambda] = eig(K_i)$  ▷  $\Psi$  contains the eigenvectors,  $\Lambda$  contains the eigenvalues
12:  if  $\Lambda(i, i) \leq tol$  then Break ▷ Truncate the eigenvalues based on  $tol$ 
13:  end if
14: end for
15:  $Q = U_i \Psi(:, 1:i-1) (\Lambda(1:i-1, 1:i-1))^{-1/2}$ 
16: return  $Q$ 

```

Algorithm 3 ROM forward solver (Algorithm 3 in [11])**Input:** $M, A, b, \Delta t, N_t, \ell = 10, tol = 1E - 14$ $\triangleright N_t = \text{ceil}(\frac{T}{\Delta t})$

```

1:  $Q = \text{get\_matrix\_Q}(M, A, b, \ell, tol)$ 
2:  $M_r = Q^T M Q, A_r = Q^T A Q, b = Q^T b$ 
3:  $u_r^0 = [0] * M_r.shape[0]$  ▷  $u_r^0$  is a zero array per (3.10)
4: Solve  $(\frac{1}{\Delta t})M_r + A_r u_r^1 = b_r, u_r = [u_r^0 | u_r^1]$ 
5: for  $i = 2$  to  $N_t$  do
6:   Solve  $(\frac{3}{2\Delta t})M_r + A_r u_r^i = \frac{1}{\Delta t}M_r(2u_r^{i-1} - \frac{1}{2}u_r^{i-2}) + b_r$ 
7:    $u_r = [u_r | u_r^i]$ 
8: end for
9: return  $Qu_r$ 

```

Using the BDF scheme in (3.5), we compose the Algorithm 3 to solve the forward process using the new ROM.

Let $N_t = \text{ceil}(\frac{T}{\Delta t})$. $Qu_r = Q[u_r^0 | u_r^1 | \dots | u_r^{N_t}]$ derived from the method above is the reduced order coefficient array projected back to the FOM. By applying this coefficient array to the finite element basis, we obtain a numerical solution to the forward process.

4 Convergence analysis and stochastic error estimate

5 Numerical results

In this section, we demonstrate the performance of our fast ROM framework in solving linear parabolic inverse source problems characterized in Section 2. We use the FEM via NGSolve package as a benchmark and find our method achieves significant computation time savings while retaining good accuracy for different source patterns¹. Our testing source functions are inspired by the work of Wang et al. (Section 5 of [12]). Our code is available at https://github.com/Readilyield/ROM_LPIS. Throughout this section, we refer the CG-FEM pipeline to the CG backward framework with FEM forward solver, and CG-ROM pipeline to the CG backward framework with our ROM forward solver.

¹All numerical results in this paper are collected by the authors using Python on a 2021 MacBook Pro with Apple M1 chip

The following table displays the setup and parameters for the testing problems. Note that our initial guess for the source term is $f_0(x, y) = \sin(\pi x)\sin(\pi y)$, which is largely irrelevant with the true source terms we have in Sections 5.1, 5.2 and 5.3.

Item	Section 5.1&5.2	Section 5.3
Ω	$[0, 1] \times [0, 1]$	$[0, 3] \times [0, 1]$
h	$1/2^8$	$1/2^7$
Δt	$1/2^8$	$1/2^7$
T	1	1
f_0	$\sin(\pi x)\sin(\pi y)$	$\sin(\pi x)\sin(\pi y)$
$tol(CG)$	$1E - 8$	$1E - 8$
λ_n	$1E - 7$	$1E - 7$
Noise level and σ	10%, $1E - 3$	10%, $1E - 3$

Table 1: General setup

5.1 Single letter reconstruction

In this part, we apply the FEM and our ROM to recover the source term f , which is an indicator function in the shape of an Arial regular font capital letter. Here we present the reconstruction of letter A. On a 5-trial average, CG-FEM uses 1018.38 seconds with 31 iterations in the CG framework (Algorithm 1) and CG-ROM uses 66.13 seconds with 72 iterations in the CG framework.

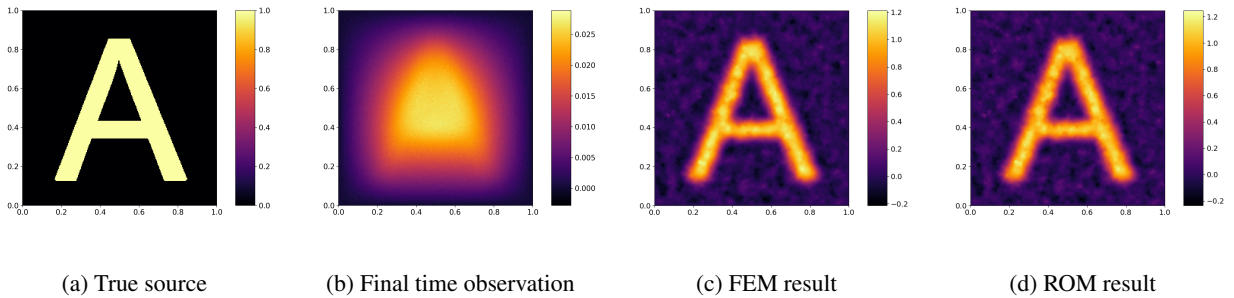


Figure 2: Letter A

5.2 Non-letter reconstruction

In this part, we apply the FEM and our ROM to recover the source term f , which is an indicator function in an irregular shape. For this example, we choose to recover a profile of Scotty, the mascot of CMU. On a 5-trial average, CG-FEM uses 1031.04 seconds with 31 iterations in the CG framework and CG-ROM uses 81.88 seconds with 97 iterations in the CG framework.

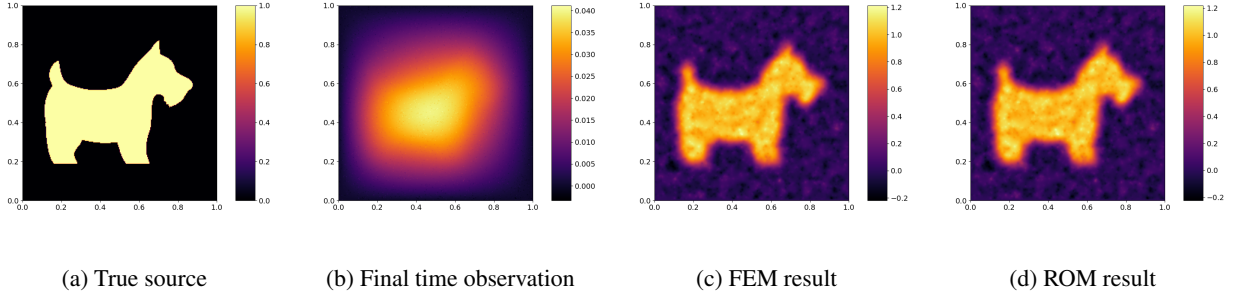


Figure 3: Scotty profile

5.3 Multiple letter reconstruction

In this part, we apply the FEM and our ROM to recover the source term f , which is an indicator function in the shape of multiple Arial regular font capital letters. Here we present the reconstruction of CMU. On a 5-trial average, CG-FEM uses 2637.18 seconds with 256 iterations in the CG framework and CG-ROM uses 171.29 seconds with 355 iterations in the CG framework.

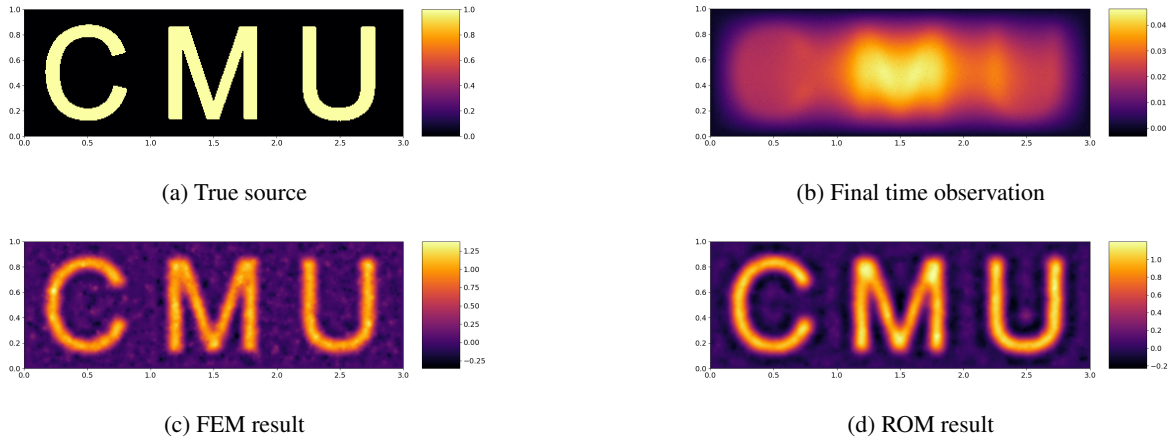


Figure 4: Letters CMU

5.4 Time efficiency gain

Here we present a table of averaged trials with varying spatial meshsize (h) and time stepsize (Δt) on recovering a single letter to demonstrate the time efficiency of our ROM. Other parameters not included in Table 2 are identical to those in Table 1. The efficiency gain is formulated as FEM time/ROM time.

h	$1/2^5$	$1/2^6$	$1/2^7$	$1/2^8$	$1/2^9$
Δt	$1/2^5$	$1/2^6$	$1/2^7$	$1/2^8$	$1/2^9$
FEM time(s)	1.98	16.07	105.51	1033.48	14416.52
ROM time(s)	0.79	3.23	15.25	60.77	364.85
Efficiency gain	2.48	4.97	6.92	17.01	39.51
FEM ite	43.0	49.0	39.0	32.0	37.0
ROM ite	77.0	96.0	93.0	70.0	62.0

Table 2: Average test results for recovering single letters

6 Concluding remarks

References

- [1] J. V. BECK, B. BLACKWELL, AND C. R. S. CLAIR JR, *Inverse heat conduction: Ill-posed problems*, James Beck, 1985.
- [2] R. BECKER, D. MEIDNER, AND B. VEXLER, *Efficient numerical solution of parabolic optimization problems by finite element methods*, *Optimisation Methods and Software*, 22 (2007), pp. 813–833.
- [3] Z. CHEN, W. ZHANG, AND J. ZOU, *Stochastic convergence of regularized solutions and their finite element approximations to inverse source problems*, *SIAM Journal on Numerical Analysis*, 60 (2022), pp. 751–780, <https://doi.org/10.1137/21M1409779>.
- [4] J. CHENG AND J. LIU, *An inverse source problem for parabolic equations with local measurements*, *Applied Mathematics Letters*, 103 (2020), p. 106213, <https://doi.org/https://doi.org/10.1016/j.aml.2020.106213>, <https://www.sciencedirect.com/science/article/pii/S0893965920300069>.
- [5] A. DE CASTRO, P. KUBERRY, I. TEZAUER, AND P. BOCHEV, *A novel partitioned approach for reduced order model—finite element model (rom-fem) and rom-rom coupling*, in *Earth and Space 2022*, ASCE Library, 2022, pp. 475–489.
- [6] M. GUBISCH AND S. VOLKWEIN, *Proper orthogonal decomposition for linear-quadratic optimal control*, *Model reduction and approximation: theory and algorithms*, 15 (2017).
- [7] C. HOMESCU, L. R. PETZOLD, AND R. SERBAN, *Error estimation for reduced-order models of dynamical systems*, *Siam Review*, 49 (2007), pp. 277–299.
- [8] T. JOHANSSON AND D. LESNIC, *Determination of a spacewise dependent heat source*, *Journal of Computational and Applied Mathematics*, 209 (2007), pp. 66–80, <https://doi.org/https://doi.org/10.1016/j.cam.2006.10.026>, <https://www.sciencedirect.com/science/article/pii/S0377042706006200>.
- [9] A. MANG, A. TOMA, T. A. SCHUETZ, S. BECKER, T. ECKEY, C. MOHR, D. PETERSEN, AND T. M. BUZUG, *Biophysical modeling of brain tumor progression: From unconditionally stable explicit time integration to an inverse problem with parabolic pde constraints for model calibration*, *Medical Physics*, 39 (2012), pp. 4444–4459.
- [10] J. L. NAZARETH, *Conjugate gradient method*, *Wiley Interdisciplinary Reviews: Computational Statistics*, 1 (2009), pp. 348–353.
- [11] N. WALKINGTON, F. WEBER, AND Y. ZHANG, *A new reduced order model of linear parabolic pdes*, 2022, <https://arxiv.org/abs/2209.11349>.
- [12] Z. WANG, W. ZHANG, AND Z. ZHANG, *A data-driven model reduction method for parabolic inverse source problems and its convergence analysis*, *Journal of Computational Physics*, 487 (2023), pp. 112–156, <https://doi.org/https://doi.org/10.1016/j.jcp.2023.112156>, <https://www.sciencedirect.com/science/article/pii/S0021999123002516>.

A Appendix

Lemma 4. *The mass matrix $M \in \mathbb{R}^{n \times n}$ is symmetric and positive definite (SPD).*

Proof. By construction, M is symmetric. So now we need to show that any non-zero vector $v \in \mathbb{R}^n$, we have

$$v^T M v > 0$$

By calculation,

$$\begin{aligned} v^T M v &= \sum_{i,j=1}^n v_i M_{ij} v_j \\ &= \sum_{i,j=1}^n v_i \left(\int_{\Omega} \phi_i \phi_j dx \right) v_j \\ &= \int_{\Omega} \left(\sum_{i=1}^n v_i \phi_i \right) \left(\sum_{j=1}^n v_j \phi_j \right) dx \end{aligned}$$

$$= \left\| \sum_{i=1}^n v_i \phi_i \right\|_{L^2(\Omega)}^2 \geq 0$$

Where $\{\phi_i\}_{i=1}^n$ is the collection of shape functions that forms a basis of the finite dimensional space V_h . Then $v^T M v = 0$ if and only if $\sum_{i=1}^n v_i \phi_i = 0$. Note that $s = \sum_{i=1}^n v_i \phi_i \in V_h$ can be viewed as a function, and $s = 0$ if and only if $v_i = 0 \forall 1 \leq i \leq n$. Since v is a non-zero vector, we conclude that $v^T M v$ must be positive. \square